Optogenetic activation of G_q signaling in astrocytes yields stimulation-specific effects on basal hippocampal synaptic excitation and inhibition

Connor D. Courtney[1], Courtney Sobieski[2,3], Charu Ramakrishnan[4], Robbie J. Ingram[1], Natalia M. Wojnowski[2], R. Anthony DeFazio[5], Karl Deisseroth[4], and Catherine A. Christian-Hinman[1,2,3*]

[1]Neuroscience Program,
[2]Department of Molecular and Integrative Physiology,
[3]Beckman Institute for Advanced Science and Technology,
University of Illinois at Urbana-Champaign, Urbana, IL 61801
[4]Department of Bioengineering, Stanford University, CA 94305
[5]Molecular and Integrative Physiology, University of Michigan, Ann Arbor, MI 48109

*Corresponding author:
Catherine A. Christian-Hinman
University of Illinois at Urbana-Champaign
407 S. Goodwin Ave.
523 Medical Sciences Building
Urbana, IL 61801, USA
E-mail: cathchri@illinois.edu

Abbreviated Title: Optogenetic stimulation of G_q in astrocytes

Acknowledgements: This work was supported by a Whitehall Foundation Research Grant, a Brain Research Foundation Fay/Frank Seed Grant, a CURE Epilepsy Taking Flight Award, NIH/NINDS grant R01 NS105825 (C.A.C.-H.), and the Beckman Institute (C.S. and N.M.W.). We thank Leanna Leverton, Lola Lozano, and Jordyn Robare for assistance with mouse colony maintenance.

Abstract:

Astrocytes play active roles at synapses and can monitor, respond, and adapt to local synaptic activity. Although there is growing evidence that astrocytes modulate synaptic excitation, the extent to which astrocytes modulate inhibition remains unknown. Additionally, tools that can selectively activate native G protein signaling pathways in astrocytes with both spatial and temporal precision are needed. Here, we present AAV8-GFAP-Optoα1AR-eYFP (Optoα1AR), an astrocyte-specific viral vector that activates the G_q-mediated intracellular cascade via light-sensitive α1-adrenergic receptors. To determine if stimulation of Optoα1AR in astrocytes modulates hippocampal synaptic transmission, whole-cell recordings were made in CA1 pyramidal cells in slices with surrounding astrocytes expressing either Optoα1AR, channelrhodopsin (ChR2), or control green fluorescent protein (GFP). CA1 astrocytes were exposed to either low-frequency (0.5 Hz, 1-s pulses at increasing 1, 5, and 10 mW intensities, 90 s/intensity) or high-frequency (20 Hz, 45-ms light pulses, 5 mW, 5 min) blue light stimulation. Low-frequency stimulation of astrocytic Optoα1AR was insufficient to modulate the frequency or strength of either inhibitory or excitatory spontaneous postsynaptic currents (sIPSCs/sEPSCs), whereas the same stimulation of astrocytic ChR2 produced increases in sIPSC frequency and sEPSC frequency and amplitude. By contrast, 20 Hz stimulation of astrocytic Optoα1AR increased frequency of both miniature IPSCs and EPSCs, and the miniature IPSC frequency effect was largely reversible within 20 min after light stimulation. These data demonstrate that Optoα1AR activation in astrocytes changes basal GABAergic and glutamatergic transmission but only following high-frequency stimulation, highlighting the importance of temporal dynamics when using optical tools to manipulate astrocyte function.

Significance statement:

Astrocytes are critical components of synapses and are known to modulate glutamatergic synaptic transmission. However, the extent to which astrocytes modulate basal GABAergic transmission is less clear. Additionally, there is demand for tools that can activate physiologically-relevant signaling pathways in astrocytes with improved temporal precision. Here, we present a novel optogenetic viral vector, AAV8-GFAP-Optoα1AR-eYFP, to stimulate astrocytes with improved temporal control. We report that high-frequency (20 Hz) stimulation of astrocytic Optoα1AR produces changes in inhibitory and excitatory transmission in hippocampal CA1, but low-frequency stimulation (0.5 Hz) is insufficient. These findings suggest that astrocytes are sensitive to the temporal dynamics of optical stimulation, and reinforce the importance of careful consideration of stimulation paradigm when using optogenetic tools to manipulate astrocytic function.

Introduction:

Astrocytes can detect synaptic signaling through G protein-coupled receptor activation (Haydon, 2001; Araque et al., 2014) and respond to local neuronal activity with transient increases in intracellular Ca^{2+} levels (Agulhon et al., 2008; Bazargani and Attwell, 2016). As influential components of the tripartite synapse, astrocytes engage in extensive and specific bidirectional communication with synapses (Araque et al., 1999; Perea et al., 2009; Santello et al., 2012). In the hippocampus, most studies investigating astrocyte-neuron interactions have demonstrated astrocyte-specific modulation of excitatory transmission and/or plasticity (Jourdain et al., 2007; Perea and Araque, 2007; Navarrete and Araque, 2010; Panatier et al., 2011; Boddum et al., 2016; Adamsky et al., 2018; Covelo and Araque, 2018; Durkee et al., 2019; Mederos et al., 2019). Evidence for astrocytic regulation of basal synaptic inhibition remains limited, although previous studies have suggested a role for astrocyte-specific modulation of synaptic inhibition in multiple brain areas including hippocampus, cortex, and thalamus (Christian and Huguenard, 2013; Mederos and Perea, 2019). For example, mechanical stimulation of astrocytes leads to glutamate release and a strengthening of inhibition that is dependent upon astrocytic Ca^{2+} signaling and AMPA/NMDA receptors (Kang et al., 1998). In addition, activation of somatostatin-positive interneurons stimulates the release of ATP/adenosine from astrocytes and subsequent enhancement of inhibition via A_1 adenosine receptors (Matos et al., 2018), suggesting that astrocytes can modulate both inhibitory and excitatory synaptic transmission.

In the hippocampus, astrocytes can sense and respond to the temporal dynamics of local interneuron activity. In hippocampal CA1, single interneuron action potentials do not alter the Ca^{2+} dynamics of local astrocytes, but interneuron burst firing drives local astrocytic Ca^{2+} transients (Perea et al., 2016). Similarly, strong stimulation of neuropeptide Y-positive interneurons in CA1 induces Ca^{2+} elevations in nearby astrocytes, but weak stimulation of these interneurons does not produce this effect

(Deemyad et al., 2018). Additional studies incorporating interneuron stimulation over 5 Hz also report intracellular increases in astrocytic Ca^{2+} (Covelo and Araque, 2018; Matos et al., 2018). Furthermore, at hippocampal CA3-CA1 synapses, astrocytes release different signaling molecules based upon the stimulation of local interneurons, such that relatively low-frequency stimulation leads to a release of astrocytic glutamate and a potentiation of synaptic glutamate release, whereas high-frequency stimulation produces astrocytic ATP/adenosine release and compensatory attenuated glutamatergic transmission (Covelo and Araque, 2018). These findings indicate that astrocytes are sensitive to the temporal frequency of local inhibitory activity and can change their functionality accordingly.

Historically, the study of neuron-astrocyte interactions has been hampered by the limited availability of tools that selectively modulate astrocytic GPCR signaling with precise spatial and temporal control. Several studies have utilized Designer Receptors Exclusively Activated by Designer Drugs (DREADDs) for specific manipulation of astrocytes (Agulhon et al., 2013; Yang et al., 2015; Chen et al., 2016; Martin-Fernandez et al., 2017; Adamsky et al., 2018). DREADDs are well-suited for this purpose as they provide targeted activation of GPCR-mediated endogenous intracellular cascades native to astrocytes. However, a limitation of DREADDs is the relative lack of temporal regulation of the activation of GPCR-mediated signaling. To overcome this drawback, in many studies the light-gated nonspecific cation channel channelrhodopsin-2 (ChR2) has been inserted into astrocyte membranes for improved temporal control (Gourine et al., 2010; Perea et al., 2014; Yamashita et al., 2014; Masamoto et al., 2015; Cui et al., 2016; Tan et al., 2017; Octeau et al., 2019). ChR2 activation, however, produces robust depolarization that likely exceeds that endogenously produced in astrocytes and increases extracellular K^+ levels (Octeau et al., 2019). Furthermore, ChR2 activation does not recapitulate a physiologically relevant signaling cascade to drive intracellular Ca^{2+} elevations in astrocytes (Xie et al., 2015). Therefore, there remains a need for optical tools that allow for precise spatial and temporal stimulation of astrocytes with

improved physiological relevance. Progress has been made in this regard with the recent development of an astrocyte-specific melanopsin coupled to the G_q intracellular pathway (Mederos et al., 2019). The use of OptoXRs (Airan et al., 2009) has emerged as another potential solution, and stimulation of Optoα1 adrenergic receptor (Optoα1AR)-derived constructs can drive Ca^{2+} elevations in cultured astrocytes (Figueiredo et al., 2014) and stimulate memory enhancement *in vivo* (Adamsky et al., 2018).

Here, we generated a novel adeno-associated virus (AAV) construct, AAV8-GFAP-Optoα1AR-eYFP, to efficiently insert light-sensitive α1-adrenergic receptors specifically into astrocytes. We report that stimulation of astrocytic Optoα1AR is sufficient to modulate basal synaptic transmission in CA1, but only when exposed to a high-frequency light stimulation. These data suggest that the temporal dynamics in which astrocytes are stimulated influence the extent of astrocytic modulation of hippocampal synaptic inhibition.

Methods:

Animals

All animal procedures were approved by the Institutional Animal Care and Use Committee of the University of Illinois at Urbana-Champaign (protocols 17161 and 20110). Male and female C57BL/6J mice were either bred on site or obtained from the Jackson Laboratory at 6-8 weeks of age. Mice were group-housed (up to five mice per cage) in a 14/10 h light:dark cycle with food and water available *ad libitum*.

Viral vectors

The pAAV-GFAP-OptoA1-eYFP plasmid was constructed by replacing the CaMKIIa promoter in pAAV-CaMKIIa-OptoA1-eYFP by a 2.2 Kb GFAP promoter and verified by Sanger sequencing. The

map and sequence information are available at web.stanford.edu/group/dlab/optogenetics/sequence_info.html#optoxr. AAV-8 (Y733F), referred to here as AAV8, was produced by the Stanford Neuroscience Gene Vector and Virus Core. In brief, AAV8-GFAP-OptoA1-eYFP was produced by standard triple transfection of AAV 293 cells (Agilent). At 72 h post-transfection, the cells were collected and lysed by a freeze-thaw procedure. Viral particles were then purified by an iodixanol step-gradient ultracentrifugation method. The iodixanol was diluted and the AAV was concentrated using a 100-kDa molecular mass–cutoff ultrafiltration device. Genomic titer was determined by quantitative PCR. The virus was tested in cultured neurons for expected expression patterns prior to use *in vivo*. AAV8-GFAP-hChR2(H134R)-eYFP and AAV8-GFAP-eGFP were obtained from the UNC Vector Core. All vectors were diluted in 0.9% sterile saline to a final titer of $1x10^{12}$ for injections; all dilutions were performed immediately prior to injection.

Stereotaxic virus injections

Stereotaxic injections were performed in mice aged postnatal day (P)42 to P90. Animals were anesthetized using 2-3% oxygen-vaporized isoflurane anesthesia (Clipper Distributing Company) and were placed in a stereotactic apparatus (Kopf Instruments). Carprofen (5 mg/kg, Zoetis) was administered subcutaneously at the beginning of surgery for analgesia. Viral vectors were loaded into a 10-µl Nanofil syringe with a 33-gauge needle, and injections were carried out using a Micro4 injection pump controller (World Precision Instruments). Viruses were bilaterally injected (1 µl per site) into dorsal hippocampal CA1 (coordinates: 1.8 mm posterior and 1.3 mm lateral to bregma; 1.3 mm ventral to the cortical surface) at a rate of 0.12 µl/min. After each injection, the syringe was left in place for 3-5 min to allow for diffusion of the viral vector and minimize reflux along the injection track. Incisions were closed using Perma-Hand

silk sutures (Ethicon). Following surgery completion, 2.5% lidocaine + 2.5% prilocaine cream (Hi-Tech Pharmacal) and Neosporin antibiotic gel (Johnson and Johnson) were applied to the incision site.

Brain slice preparation

Acute brain slices were prepared at ages P80-P145, with a range of 26-71 days after stereotaxic virus injection. Mice were anesthetized via intraperitoneal injection of pentobarbital (Vortech Pharmaceuticals, 55 mg/kg) and euthanized by decapitation. Brains were immediately dissected and placed in an ice-cold oxygenated (95% O_2/5% CO_2) high-sucrose slicing solution containing (in mM) 254 sucrose, 11 glucose, 2.5 KCl, 1.25 NaH_2PO_4, 10 $MgSO_4$, 0.5 $CaCl_2$, and 26 $NaHCO_3$. 300 µm-thick coronal slices through dorsal hippocampus were prepared using a Leica VT1200S vibratome (Leica Biosystems). Slices were hemisected, transferred to a holding chamber, and incubated in an oxygenated artificial cerebrospinal fluid (ACSF) solution containing (in mM) 126 NaCl, 2.5 KCl, 10 glucose, 1.25 NaH_2PO_4, 1 $MgSO_4$, 2 $CaCl_2$, and 26 $NaHCO_3$ at ~298 mOsm. For all experiments, slices were incubated in ACSF for 60 min at 32°C, then moved to room temperature (21-23°C) for at least 15 min before recording.

Patch clamp electrophysiology

Slices were placed in a fully submerged recording chamber on the stage of an upright BX51WI microscope (Olympus America) and continuously superfused with oxygenated ACSF at a rate of 2.5 ml/min at room temperature. Recordings were made using a MultiClamp 700B amplifier, Digidata 1550 digitizer, and Clampex 10 software (Molecular Devices). Recording pipettes were prepared from thick-walled borosilicate glass using a P-1000 micropipette puller (Sutter Instruments). For all experiments, access resistance was monitored every 2-5 minutes. Only cells that displayed a low and stable access

resistance (R_a <20 MΩ; <20% change in R_a for the duration of the experiment) were kept for analyses. There were no differences between groups in access resistance, input resistance, or cell capacitance.

For voltage-clamp recordings, pipettes were pulled to have an open-tip resistance of 2-5 MΩ when filled with an internal solution containing (in mM): 130 Cs-gluconate, 8 CsCl, 2 NaCl, 10 HEPES, 4 EGTA, 4 Mg-ATP, 0.3 GTP, adjusted to 290 mOsm and pH 7.3. Individual neurons were selected for their pyramidal shape using differential infrared contrast optics through either a sCMOS camera (OrcaFlash 4.0LT, Hamamatsu) or a Retiga R1 CCD camera (Teledyne Photometrics). Slices were screened for GFP expression by brief epifluorescence illumination at 470 nm, and only neurons with nearby astrocytes displaying fluorescence were subsequently recorded. Excitatory and inhibitory postsynaptic currents (EPSCs/IPSCs) were recorded in the absence of synaptic blockers. EPSCs were recorded at a membrane holding potential (V_m) of -70 mV, whereas IPSCs were recorded at V_m = 0 mV. The efficacy of this recording paradigm in isolating EPSCs and IPSCs, respectively, was confirmed by the abolishment of currents following application of glutamate receptor blockers APV and DNQX with V_m = -70 mV, as well as the abolishment of currents following application of the $GABA_A$ receptor blocker picrotoxin with V_m = 0 mV. Each cell was randomly assigned for recording of either EPSCs or IPSCs. Only one cell was recorded per slice. For miniature PSC (mEPSC/mIPSC) recordings, 0.5 µM tetrodotoxin (TTX, Abcam) was added to the bath ACSF. For optogenetic activation, 473 nm blue laser light (Laserglow Technologies) was delivered through an optical fiber 200 µm in diameter (FT200EMT, Thorlabs) placed directly above stratum radiatum/stratum pyramidale at the surface of the slice. Two stimulation paradigms were used: 1) 0.5 Hz (1-s pulses at successive 1, 5, and 10 mW intensities, 90-s duration per intensity, 50% duty cycle); 2) 20 Hz (45-ms pulses at 5 mW intensity, 5 min in duration, 90% duty cycle; partially adapted from *in vivo* experiments in Adamsky et al., 2018).

Immunohistochemistry

At 3 weeks after injection, animals were euthanized via intracardiac perfusion with 20 mL of 0.1M PBS, followed by 20 mL of 4% paraformaldehyde (PFA). Tissue was then collected, fixed in 4% PFA for 24 h at 4°C, and preserved in 30% sucrose solution with 0.5% sodium azide until sectioning. 40 µm-thick coronal sections were prepared using a freezing microtome (SM 2010R, Leica Biosystems). Hippocampal sections were washed 3 times with 0.01 M PBS for 5 min each at room temperature on a shaker at 140 rpm, then incubated for 1 h in a tris-buffered saline (TBS)-based blocking solution (10% normal donkey serum, 0.1% Triton X-100, 2% bovine serum albumin). Sections were then incubated with primary antibody (anti-NeuN rabbit polyclonal [1:1000, Sigma ABN78]) for 48 h at 4°C on a shaker. Sections were then washed in PBS and incubated with DyLight 594-conjugated goat anti-rabbit secondary antibody (anti-rabbit [1:1000, Vector Laboratories DI-1594) for 2 h on a shaker at room temperature. Tissue was mounted on charged glass slides and coverslipped using Vectashield Hardset Antifade Mounting Medium with DAPI (Vector Laboratories, H-1500). Imaging acquisition was performed using a BX43 light and fluorescence microscope equipped with a Q-Color 3 camera (Olympus) and QCapture Pro 7 software (Teledyne Photometrics).

Data analysis and statistics

Postsynaptic currents were analyzed using Stimfit software (Guzman et al., 2014) or a custom analysis package in IGOR Pro (WaveMetrics) (DeFazio et al., 2014). Passive electrical properties were calculated using Clampfit 10.4 (Molecular Devices). Data from Stimfit/IGOR were transferred to OriginPro 2016 (OriginLab, Northampton, MA, USA) or RStudio for statistical analysis. Comparisons for 0.5 Hz stimulation experiments were made using two-way repeated-measures ANOVA (opsin and stimulation intensity as factors) with Tukey's post-hoc tests. Within-group comparisons for the 20 Hz

stimulation experiments (before/after light stimulation) were made using paired t-tests. 20 Hz mIPSC recordings with baseline, light, and 20-min post-light timepoints were analyzed using one-way repeated-measures ANOVA (with time as the repeated factor) with Tukey's post-hoc tests. Pearson's correlation coefficient (r) was used to measure the linear correlation between tonic current amplitude and EPSC frequency. $P<0.05$ was considered statistically significant.

Results:

Astrocyte-specific expression of optogenetic constructs

AAV8 vectors driven by the astrocyte-specific GFAP promoter were individually injected into dorsal CA1 of wild-type C57BL/6J mice. For each mouse, one of three constructs was used: GFAP-Optoα1AR-eYFP (Optoα1AR), GFAP-hChR2(H134R)-eYFP (ChR2), and GFAP-GFP (GFP). To confirm the astrocyte-specificity of these vectors, immunohistochemistry was performed for the neuronal marker NeuN. Colocalization was not observed between NeuN staining of CA1 pyramidal cells and the GFP or eYFP fluorescent tags of any AAV used (**Figure 1**), indicating a lack of neuronal expression of the optogenetic constructs.

Low-frequency (0.5 Hz) optogenetic stimulation of astrocytic ChR2, but not Optoα1AR, modulates hippocampal synaptic inhibition

To examine the effect of local astrocyte activation on basal synaptic transmission in hippocampus, whole-cell patch clamp recordings of spontaneous inhibitory or excitatory postsynaptic currents (sIPSCs/sEPSCs) were made in CA1 pyramidal cells. For optical stimulation of astrocytes, we devised a prolonged, low-frequency paradigm designed to resemble the slower kinetics of GPCR signaling cascades as compared to ionic membrane conductances. To investigate the impacts of low-frequency stimulation

of the opsins, slices containing astrocytes expressing either Optoα1AR, ChR2, or control GFP were exposed to 0.5 Hz blue light stimulation at successive 1, 5, or 10 mW intensities for 90 s per intensity, with 2 min between stimulations (**Figure 2A**). First, we investigated the impact of 0.5 Hz activation of Optoα1AR, ChR2, or GFP in astrocytes in modulating hippocampal inhibitory transmission (henceforth referred to as Optoα1AR, ChR2, and GFP groups for simplicity). Following 0.5 Hz stimulation of slices in the Optoα1AR group, there was no change in sIPSC frequency compared to baseline at any stimulation intensity timepoint (**Figure 2B and 2C, middle**) (n=10 cells from 6 mice). Additionally, there was no difference in sIPSC frequency in response to light stimulation between the Optoα1AR and GFP groups (**Figure 2B and 2C, top**) (GFP n=10 cells from 4 mice). However, the ChR2 group displayed a robust increase in IPSC frequency following 1 mW-intensity stimulation compared to baseline ($p=0.002$) (n=7 cells from 4 mice), as well as compared to the GFP group at 1 mW and 5 mW ($p<0.001$, respectively) (**Figure 2B and 2C, bottom**). Notably, the strength of this ChR2-mediated effect diminished over time despite an increase in stimulation intensity; there was no significant difference compared to baseline at 5 mW intensity, nor compared to either baseline or to the GFP group at 10 mW stimulation, indicating a potent rundown of the effect within minutes that increased light intensity did not overcome. Furthermore, no differences were detected in sIPSC amplitude in any experimental group at any stimulation intensity ($F=0.76$, $p=0.55$) (**Figure 2D**). Together, these data indicate that 0.5 Hz optogenetic stimulation of the nonspecific cation channel ChR2 in astrocytes modulates sIPSC frequency in CA1 hippocampal pyramidal cells, but the same stimulation of Optoα1AR to trigger the G_q signaling cascade in astrocytes is insufficient.

Low-frequency (0.5 Hz) optogenetic stimulation of astrocytic ChR2, but not Optoα1AR, modulates hippocampal glutamatergic transmission

Previous studies using G_q-coupled optogenetic or chemogenetic tools have demonstrated that activation of this pathway in astrocytes can modulate basal excitatory neurotransmission in the hippocampus (Adamsky et al., 2018; Mederos et al., 2019). To determine if low-frequency 0.5 Hz stimulation modulates glutamatergic transmission in the hippocampus, sEPSCs were recorded from CA1 pyramidal cells (**Figure 3A**). Similar to the data for sIPSCs, 0.5 Hz stimulation of slices in the Optoα1AR group did not result in an overall difference in sEPSC frequency compared to baseline at any stimulation intensity (**Figure 3B, middle**) (n=10 cells from 5 mice). In addition, no differences in sEPSC frequency were detected between the Optoα1AR and GFP groups at any stimulation intensity timepoint (**Figure 3B, top**) (GFP n=10 cells from 4 mice). However, as with sIPSCs, the ChR2 group displayed a potent increase in sEPSC frequency following 1 mW stimulation as compared to baseline ($p=0.04$), and compared to GFP controls at both 1 mW ($p<0.001$) and 5 mW intensities ($p=0.02$) (n=9 cells from 4 mice) (**Figure 3B, bottom**). This effect also diminished over time, with no difference in response to 10 mW stimulation compared to baseline or compared to control GFP. However, in contrast to the findings for sIPSCs, analysis of sEPSC amplitude with 0.5 Hz stimulation yielded significant effects at 1 mW ($p=0.03$) and 10 mW ($p<0.001$) intensities compared to GFP controls (**Figure 3C**). These data indicate that low-frequency 0.5 Hz blue light stimulation does not modulate basal excitatory synaptic transmission in CA1 pyramidal cells when Optoα1AR is expressed in astrocytes, but in the case of astrocytic ChR2, this same stimulation produces increased sEPSC frequency and amplitude.

In 5 of 9 recorded cells, 0.5 Hz stimulation of ChR2 in astrocytes when recording sEPSCs also resulted in the development of an inward tonic current that did not appear when recording sIPSCs**.** Furthermore, this ChR2-mediated tonic current displayed two unique temporal profiles: a slow tonic

current that peaked in amplitude during the first 30 s of 0.5 Hz light exposure (**Figure 4A, top**); and an acute tonic current that fluctuated with the on/off stimulation of the light (**Figure 4A, middle and bottom**). The amplitude of the slow tonic current ranged from 31.98-191.71 pA, with a mean time to peak amplitude of 15.09 s following 1 mW 0.5 Hz stimulation (**Figure 4B**). The acute tonic current was largest during the initial 10 s of 0.5 Hz light stimulation (mean 43.61 $\pm$ 20.81 pA), but recovered to 47.54% of max amplitude within 30 s of stimulation (mean 22.88 $\pm$ 6.96 pA) (**Figure 4C**). Additionally, a strong linear correlation was observed between the amplitude of the slow tonic current and phasic sEPSC frequency, as cells with the highest phasic sEPSC frequency displayed the greatest amplitude of the slow tonic current ($r=0.99$, $p<0.0001$) (**Figure 4D**).

High-frequency (20 Hz) optogenetic stimulation of Optoα1AR in astrocytes yields a trend towards increased frequency and decreased amplitude of sIPSCs

In the hippocampus, the specific signaling molecules released by astrocytes depend on the firing frequencies of local neuronal activity (Covelo and Araque, 2018), and high-frequency (20 Hz) stimulation of a similar OptoG_q construct in CA1 astrocytes improves memory performance *in vivo* (Adamsky et al., 2018). Therefore, we sought to determine if the temporal properties of astrocytic Optoα1AR stimulation are critical in shaping the modulation of hippocampal synaptic transmission. Whole-cell recordings were made in CA1 pyramidal cells with nearby astrocytes expressing either Optoα1AR, ChR2, or GFP as before, but with slices exposed to high-frequency (20 Hz) blue-light stimulation at a consistent 5 mW intensity for 5 min (closely resembling the *in vivo* experiments from Adamsky et al., 2018) (**Figure 5A-5B**). Analysis of sIPSCs from the Optoα1AR group indicated a trend towards increased frequency during the 20 Hz light stimulation compared to baseline ($t=-1.91$, $p=0.07$, $n=16$ cells from 5 mice) (**Figure 5C**), and there were no differences in sIPSC frequency in the control GFP group ($t=0.67$, $p=0.51$, $n=8$ cells

from 2 mice) **(Figure 5C)**. sIPSCs from the Optoα1AR group also displayed a trend towards decreased amplitude (t=1.77, p=0.09), an effect not seen in GFP controls (t=-0.01, p=0.99) (**Figure 5D**).

High-frequency (20 Hz) optogenetic stimulation of Optoα1AR in astrocytes modulates activity-independent hippocampal synaptic inhibition

Although the effects on the sIPSC properties with 20 Hz stimulation of astrocytic Optoα1AR did not reach statistical significance, the trends seen in the data were intriguing enough to warrant further investigation. Therefore, mIPSCs were recorded under the same stimulation paradigm in the presence of tetrodotoxin (TTX, 0.5 μM) to prevent action potential firing (**Figure 6A**). mIPSCs recorded from the Optoα1AR group displayed an increase in frequency in response to light stimulation (t=-3.51, p=0.004, n=14 cells from 6 mice). This effect was not seen in the control GFP group (t=-0.84, p=0.42, n=13 cells from 5 mice) (**Figure 6B**), suggesting that 20 Hz stimulation of Optoα1AR can acutely elicit an activity-independent mechanism producing increased frequency of GABA release onto CA1 pyramidal cells. mIPSC amplitude was not affected by light stimulation in the Optoα1AR group (t=-0.96, p=0.35) (**Figure 6C**), in contrast to the trend towards a decrease in sIPSC amplitude in response to the same stimulation, suggesting the possibility of an action potential-dependent reduction in sIPSC amplitude. Unexpectedly, there was a significant increase in mIPSC amplitude in cells from the GFP group (t=-4.10, p<0.001) (**Figure 6C**). This result likely reflects the smaller baseline amplitude of currents in cells from the GFP group (mean 17.55 ± 0.62 pA) in comparison to the baseline amplitude of currents in cells from the Optoα1AR group (mean 19.55 ± 0.41 pA; p=0.02). However, the mean amplitude of events during the light stimulation was similar between groups.

An important advantage of using optogenetic tools is the temporal precision of activation (Deisseroth, 2015), and Optoα1AR expression in neurons allows for spatiotemporally precise

manipulation of biochemical signaling and modulation of behavior *in vivo* (Airan et al., 2009). In theory, this temporal control potentially allows cellular modulation to be reversible at short timescales. To test this possibility, we recorded mIPSCs in a subset of cells in slices expressing Optoα1AR or GFP in astrocytes for 20 additional min following cessation of the 20 Hz light stimulation. In these cells, mIPSC frequency was increased during the initial 20 Hz stimulation of Optoα1AR compared to baseline, similar to the change in mIPSC frequency observed in the full group as shown in Figure 6 (p=0.01). However, there was no longer a significant difference in mIPSC frequency at 20 min post-stimulation compared to baseline (p=0.16) (n=9 cells from 6 mice) (**Figure 7A**). A decrease in mIPSC frequency at 20 min compared to the time of light stimulation was seen in 6 of 9 cells, and 5 of those 6 cells displayed a reduction of at least 50% compared to peak frequency recorded during the light stimulation. This finding suggests that the increase in mISPC frequency was largely reversible within 20 min following high-frequency stimulation of astrocytic Optoα1AR. In cells from the GFP group, by contrast, no change in mIPSC frequency was seen either during the 20 Hz stimulation or at 20 min afterwards (n=9 cells from 4 mice) (**Figure 7A**). Additionally, there were no significant changes in mIPSC amplitude during the light stimulation or at 20 min afterwards in cells from either the Optoα1AR or GFP groups (**Figure 7B**). Altogether, these data indicate that high-frequency 20 Hz stimulation of Optoα1AR in astrocytes transiently modulates basal inhibitory transmission in CA1 pyramidal cells, an effect that largely dissipates within a 20-min time period.

High-frequency (20 Hz) optogenetic stimulation of Optoα1AR in astrocytes modulates activity-independent hippocampal glutamatergic transmission

Although low-frequency 0.5 Hz stimulation of Optoα1AR in astrocytes did not alter glutamatergic synaptic transmission, we hypothesized that high-frequency stimulation would be efficacious given the

observed effects of this stimulation on synaptic inhibition. To determine if high-frequency 20 Hz stimulation is sufficient to modulate hippocampal glutamatergic transmission, mEPSCs were recorded from CA1 pyramidal cells (**Figure 8A**). This stimulation produced an increase in mEPSC frequency compared to baseline in the Optoα1AR group (t=-3.68, p=0.005, n=10 cells from 4 mice), and this effect was not observed in the control GFP group (t=0.13, p=0.91, n=6 cells from 4 mice) (**Figure 8B**). Additionally, mEPSC amplitude was not changed with 20 Hz stimulation in either the Optoα1AR (t=-1.38, p=0.20) or GFP groups (t=-0.63, p=0.56) (**Figure 8C**).

Discussion:

In these studies, we employed the G_q-coupled opsin, Optoα1AR, expressed in astrocytes to investigate astrocytic modulation of basal synaptic transmission in hippocampal CA1. Our results indicate that optical stimulation of astrocytic Optoα1AR is capable of modulating synaptic transmission, including basal GABAergic inhibition, in hippocampus. Furthermore, these effects are stimulation-specific; only high-frequency (20 Hz) stimulation of Optoα1AR in astrocytes effectively modulated hippocampal transmission. Low-frequency 0.5 Hz stimulation of Optoα1AR had no effect on modulating hippocampal IPSCs or EPSCs, in stark contrast to the large changes seen with low-frequency stimulation of astrocytes expressing the nonspecific cation channel ChR2. 20 Hz stimulation of astrocytic Optoα1AR led to increases in both mIPSC and mEPSC frequency, and the increase in mIPSC frequency was largely reversible within 20 min. Altogether, we offer evidence for stimulation-specific effects of astrocytes in modulating both GABAergic and glutamatergic transmission in hippocampal CA1 and urge future studies to carefully consider the nature of the optical stimulation paradigms when using optogenetic tools to target astrocytes.

Currently, the G_q-coupled DREADD, hM3Dq (Roth, 2016), is the most commonly used tool for targeted activation of astrocytes due to its ease of use and physiological relevance when inserted into astrocytes and activated by clozapine-N-oxide (CNO) or other similar ligand. The Optoα1AR vector employed here may be used as an alternative to hM3Dq for astrocyte stimulation by activating the same endogenous pathway with improved temporal specificity. As CNO is typically administered over an extended period of time, and the effects of hM3Dq activation can be long-lasting, one must consider the temporal incongruence between experiments that activate astrocytes using DREADDs versus optogenetic tools. The present study highlights the importance of the frequency and duration of optical stimulation paradigms when using optogenetic constructs to interrogate roles for astrocytes in modulating synaptic transmission. For example, in a prior study, sustained optical stimulation of CA1 astrocytes expressing G_q-coupled melanopsin at 7 mW for 1 s or 3 s was insufficient to modulate sEPSCs. However, stimulation lengths of 5 s and 10 s led to transient increases in sEPSC amplitude, and stimulation lengths of 20 s and 60 s induced sustained increases in sEPSC amplitude (Mederos et al., 2019). The effects on excitatory transmission observed here in response to 20 Hz, 5 mW stimulation of Optoα1AR are in line with these previously described effects of astrocyte-expressed melanopsin, and extend the effects of activation of G_q signaling in astrocytes to modulation of synaptic inhibition as well. In the present studies, however, 0.5 Hz stimulation (repeated 1-s light pulses delivered over 90 s) of astrocytic Optoα1AR at intensities up to 10 mW did not alter EPSC frequency or amplitude as compared to stimulation of control GFP, suggesting that unsustained, low-frequency stimulation of G_q signaling in astrocytes is insufficient to modulate hippocampal transmission. It is possible that the escalating-intensity stimulation paradigm used in the present studies masked a potential effect of the higher intensity light stimulations. In addition, it is important to note that the stimulation paradigms used in these experiments are just two of many possible options. The 0.5 Hz stimulation paradigm was designed in an attempt to mimic the relatively slow

activation kinetics of astrocytic GPCRs, as well as the temporal dynamics of astrocytic Ca^{2+} signaling, which are generally seconds in length (Haustein et al., 2014; Srinivasan et al., 2015). It should be noted, however, that recent work has identified Ca^{2+} signals in astrocyte microdomains with ms timescales *in vivo* (Stobart et al., 2018). By contrast, the 20 Hz stimulation was chosen to better represent the timescale of neuronal activity in the hippocampus, as well as to closely mimic light delivery used in previous *in vivo* experiments (Adamsky et al., 2018).

The present study reports direct modulation of basal synaptic inhibition by astrocytes using an optogenetic tool designed to harness physiologically relevant endogenous pathways in astrocytes. High-frequency stimulation of Optoα1AR in astrocytes resulted in elevated mIPSC frequency, which suggests a potential Ca^{2+}-dependent release of a signaling molecule from astrocytes that acts upon presynaptic terminals of interneurons, subsequently increasing the probability of GABA release at inhibitory synapses. As mIPSC amplitude was not changed, quantal size does not appear to have been affected. Purinergic signaling is potential mediator of this response; astrocytes release ATP/adenosine in a Ca^{2+}-dependent manner, and ATP/adenosine has been shown to modulate both basal excitatory neurotransmission (Di Castro et al., 2011; Panatier et al., 2011) as well as heterosynaptic depression (Serrano et al., 2006; Andersson et al., 2007; Boddum et al., 2016) in the hippocampus. Purinergic signaling can also modulate inhibitory transmission; for example, endogenous $P2Y_1$ receptor activation in hippocampal interneurons leads to increased interneuron excitability, subsequently increasing feed-forward inhibition onto CA1 pyramidal cells. Both anatomical and functional evidence (a high density of astrocyte processes surrounding hippocampal interneurons and enhanced intracellular Ca^{2+} transients, respectively) suggests that these effects are driven by astrocyte-derived ATP (Bowser and Khakh, 2004). Additionally, astrocytic release of ATP/adenosine upregulates synaptic inhibition from somatostatin interneurons onto pyramidal cells in the hippocampus (Matos et al., 2018). Furthermore, in the central amygdala, G_q pathway

stimulation in astrocytes leads to Ca^{2+}-dependent release of ATP/adenosine and an enhancement of inhibition through activation of neuronal $A2_A$ receptors (Martin-Fernandez et al., 2017). These effects were deemed to be mediated presynaptically, in line with the increased mIPSC frequency seen in the present studies. It remains unclear, however, why increased IPSC frequency was only observed when action potential firing was blocked. It is important to note that all recordings in this study were made in the absence of synaptic blockers; EPSCs and IPSCs were biophysically isolated only in the recorded cell. Though recordings made from slices in the absence of synaptic blockers may be more representative of *in vivo* conditions, the recordings represent the net result of both excitatory and inhibitory network activity, making the underlying mechanisms difficult to pinpoint. In addition, other potential mechanisms may be considered. For example, astrocytes provide metabolic support to neurons, and disruption of metabolic processes such as glycolysis and oxidative phosphorylation can alter presynaptic vesicular release (Sobieski et al., 2017). Future studies should also consider the potential impact that optical tools may have on the important metabolic roles of astrocytes.

Low-frequency stimulation of ChR2 in astrocytes not only altered phasic synaptic excitation but produced a tonic inward current as well. Of note, a similar slow inward current with superimposed sEPSCs has also been shown after ChR2 activation in astrocytes in the striatum (Cui et al., 2016). Mechanistically, the tight correlation between tonic current amplitude and sEPSC frequency in the presence of light stimulation suggests that stimulation of ChR2 in astrocytes causes the release of glutamate from astrocytic stores, flooding synaptic clefts with glutamate and increasing synaptic EPSC frequency at least in part via increased binding events onto postsynaptic ionotropic glutamate receptors. Subsequent glutamate spillover then drives the tonic inward current, possibly via activation of extrasynaptic NMDA receptors (Angulo et al., 2004; Fellin et al., 2004; Le Meur et al., 2007), which can be activated despite a hyperpolarized holding potential and the presence of Mg^{2+} in the extracellular solution (Fellin et al., 2004).

The present study used a novel variant of Optoα1AR (Airan et al., 2009) packaged in AAV8 and driven by a GFAP promoter for astrocyte-specificity. Optoα1AR canonically drives Ca^{2+} elevations via activation of endogenous G_q, leading to the release of Ca^{2+} from IP_3-dependent intracellular stores, as previously demonstrated both in HEK cells (Airan et al., 2009) and cultured astrocytes (Figueiredo et al., 2014). Therefore, it is unlikely that the present results are due to a Ca^{2+}-independent mechanism triggered in the astrocytes. One potential explanation for the stimulation-specific modulation of hippocampal synaptic transmission seen here is that the 0.5 Hz stimulation of Optoα1AR may be insufficient to drive consistent increases in astrocytic intracellular Ca^{2+} levels as compared to the high-frequency 20 Hz stimulation, thus failing to trigger Ca^{2+}-dependent release of signaling molecules. Future studies using the Optoα1AR construct could compare the properties of astrocytic Ca^{2+} elevations following exposure to varying stimulation paradigms.

In summary, the goal of these experiments was to investigate roles for astrocytes in the modulation of basal synaptic transmission using the novel optogenetic construct GFAP-Optoα1AR. Our data indicate that light activation of Optoα1AR in astrocytes effectively modulates basal synaptic inhibition as well as synaptic excitation in the hippocampus, but that this modulation requires high-frequency blue light delivery. Low-frequency 0.5 Hz stimulation of astrocytic Optoα1AR was insufficient to modulate glutamatergic or GABAergic transmission across a range of light intensities, although this stimulation produced robust responses when ChR2 was expressed in astrocytes. Overall, this work suggests that careful consideration should be made when determining the frequency and intensity of optical stimulation used in future studies employing optogenetic tools to probe and manipulate glial-neuronal interactions, along with the potential physiological relevance of such stimulation paradigms.

References:

Adamsky A, Kol A, Kreisel T, Doron A, Ozeri-Engelhard N, Melcer T, Refaeli R, Horn H, Regev L, Groysman M, London M, Goshen I (2018) Astrocytic Activation Generates De Novo Neuronal Potentiation and Memory Enhancement. Cell 174:59-71.e14.

Agulhon C, Boyt KM, Xie AX, Friocourt F, Roth BL, McCarthy KD (2013) Modulation of the autonomic nervous system and behaviour by acute glial cell Gq protein-coupled receptor activation in vivo. J Physiol 591:5599–5609.

Agulhon C, Petravicz J, McMullen AB, Sweger EJ, Minton SK, Taves SR, Casper KB, Fiacco TA, McCarthy KD (2008) What is the role of astrocyte calcium in neurophysiology? Neuron 59:932–946.

Airan RD, Thompson KR, Fenno LE, Bernstein H, Deisseroth K (2009) Temporally precise in vivo control of intracellular signalling. Nature 458:1025–1029.

Andersson M, Blomstrand F, Hanse E (2007) Astrocytes play a critical role in transient heterosynaptic depression in the rat hippocampal CA1 region. J Physiol 585:843–852.

Angulo MC, Kozlov AS, Charpak S, Audinat E (2004) Glutamate released from glial cells synchronizes neuronal activity in the hippocampus. J Neurosci 24:6920–6927.

Araque A, Carmignoto G, Haydon PG, Oliet SHR, Robitaille R, Volterra A (2014) Gliotransmitters travel in time and space. Neuron 81:728–739.

Araque A, Parpura V, Sanzgiri RP, Haydon PG (1999) Tripartite synapses: glia, the unacknowledged partner. Trends Neurosci 22:208–215.

Bazargani N, Attwell D (2016) Astrocyte calcium signaling: the third wave. Nat Neurosci 19:182–189.

Boddum K, Jensen TP, Magloire V, Kristiansen U, Rusakov DA, Pavlov I, Walker MC (2016) Astrocytic GABA transporter activity modulates excitatory neurotransmission. Nat Commun 7:13572.

Bowser DN, Khakh BS (2004) ATP excites interneurons and astrocytes to increase synaptic inhibition in neuronal networks. J Neurosci 24:8606–8620.

Chen N, Sugihara H, Kim J, Fu Z, Barak B, Sur M, Feng G, Han W (2016) Direct modulation of GFAP-expressing glia in the arcuate nucleus bi-directionally regulates feeding. Elife 5:e18716.

Christian CA, Huguenard JR (2013) Astrocytes potentiate GABAergic transmission in the thalamic reticular nucleus via endozepine signaling. Proc Natl Acad Sci 110:20278–20283.

Covelo A, Araque A (2018) Neuronal activity determines distinct gliotransmitter release from a single astrocyte. Elife 7:e32237.

Cui Q, Pitt JE, Pamukcu A, Poulin JF, Mabrouk OS, Fiske MP, Fan IB, Augustine EC, Young KA, Kennedy RT, Awatramani R, Chan CS (2016) Blunted mGluR Activation Disinhibits Striatopallidal Transmission in Parkinsonian Mice. Cell Rep 17:2431–2444.

Deemyad T, Lüthi J, Spruston N (2018) Astrocytes integrate and drive action potential firing in inhibitory subnetworks. Nat Commun 9:4336-.

DeFazio RA, Elias CF, Moenter SM (2014) Gabaergic transmission to kisspeptin neurons is differentially regulated by time of day and estradiol in female mice. J Neurosci 34:16296–16308.

Deisseroth K (2015) Optogenetics: 10 years of microbial opsins in neuroscience. Nat Neurosci 18:1213–1225.

Di Castro MA, Chuquet J, Liaudet N, Bhaukaurally K, Santello M, Bouvier D, Tiret P, Volterra A (2011) Local Ca2+detection and modulation of synaptic release by astrocytes. Nat Neurosci 14:1276–1284.

Durkee CA, Covelo A, Lines J, Kofuji P, Aguilar J, Araque A (2019) G i/o protein-coupled receptors

inhibit neurons but activate astrocytes and stimulate gliotransmission. Glia 67:1076–1093.
Fellin T, Pascual O, Gobbo S, Pozzan T, Haydon PG, Carmignoto G (2004) Neuronal synchrony mediated by astrocytic glutamate through activation of extrasynaptic NMDA receptors. Neuron 43:729–743.
Figueiredo M, Lane S, Stout Jr RF, Liu B, Parpura V, Teschemacher AG, Kasparov S (2014) Comparative analysis of optogenetic actuators in cultured astrocytes. Cell Calcium 56:208–214.
Gourine A V., Kasymov V, Marina N, Tang F, Figueiredo MF, Lane S, Teschemacher AG, Spyer KM, Deisseroth K, Kasparov S (2010) Astrocytes control breathing through pH-dependent release of ATP. Science 329:571–575.
Guzman SJ, Schlögl A, Schmidt-Hieber C (2014) Stimfit: quantifying electrophysiological data with Python. Front Neuroinform 8:16.
Haustein MD, Kracun S, Lu XH, Shih T, Jackson-Weaver O, Tong X, Xu J, Yang XW, O'Dell TJ, Marvin JS, Ellisman MH, Bushong EA, Looger LL, Khakh BS (2014) Conditions and constraints for astrocyte calcium signaling in the hippocampal mossy fiber pathway. Neuron 82:413–429.
Haydon PG (2001) GLIA: listening and talking to the synapse. Nat Rev Neurosci 2:185.
Jourdain P, Bergersen LH, Bhaukaurally K, Bezzi P, Santello M, Domercq M, Matute C, Tonello F, Gundersen V, Volterra A (2007) Glutamate exocytosis from astrocytes controls synaptic strength. Nat Neurosci 10:331–339.
Kang J, Jiang L, Goldman SA, Nedergaard M (1998) Astrocyte-mediated potentiation of inhibitory synaptic transmission. Nat Neurosci 1:683–692.
Le Meur K, Galante M, Angulo MC, Audinat E (2007) Tonic activation of NMDA receptors by ambient glutamate of non-synaptic origin in the rat hippocampus. J Physiol 580:373–383.
Martin-Fernandez M, Jamison S, Robin LM, Zhao Z, Martin ED, Aguilar J, Benneyworth MA, Marsicano G, Araque A (2017) Synapse-specific astrocyte gating of amygdala-related behavior. Nat Neurosci 20:1540–1548.
Masamoto K, Unekawa M, Watanabe T, Toriumi H, Takuwa H, Kawaguchi H, Kanno I, Matsui K, Tanaka KF, Tomita Y (2015) Unveiling astrocytic control of cerebral blood flow with optogenetics. Sci Rep 5:11455.
Matos M, Bosson A, Riebe I, Reynell C, Vallée J, Laplante I, Panatier A, Robitaille R, Lacaille JC (2018) Astrocytes detect and upregulate transmission at inhibitory synapses of somatostatin interneurons onto pyramidal cells. Nat Commun 9:4254.
Mederos S, Hernández-Vivanco A, Ramírez-Franco J, Martín-Fernández M, Navarrete M, Yang A, Boyden ES, Perea G (2019) Melanopsin for precise optogenetic activation of astrocyte-neuron networks. Glia 67:915–934.
Mederos S, Perea G (2019) GABAergic-astrocyte signaling: A refinement of inhibitory brain networks. Glia 67:1842–1851.
Navarrete M, Araque A (2010) Endocannabinoids potentiate synaptic transmission through stimulation of astrocytes. Neuron 68:113–126.
Octeau JC, Gangwani MR, Allam SL, Tran D, Huang S, Hoang-Trong TM, Golshani P, Rumbell TH, Kozloski JR, Khakh BS (2019) Transient, Consequential Increases in Extracellular Potassium Ions Accompany Channelrhodopsin2 Excitation. Cell Rep 27:2249-2261.e7.
Panatier A, Vallée J, Haber M, Murai KK, Lacaille JC, Robitaille R (2011) Astrocytes are endogenous regulators of basal transmission at central synapses. Cell 146:785–798.
Perea G, Araque A (2007) Astrocytes potentiate transmitter release at single hippocampal synapses. Science 317:1083–1086.
Perea G, Gómez R, Mederos S, Covelo A, Ballesteros JJ, Schlosser L, Hernández-Vivanco A, Martín-

Fernández M, Quintana R, Rayan A, Díez A, Fuenzalida M, Agarwal A, Bergles DE, Bettler B, Manahan-Vaughan D, Martín ED, Kirchhoff F, Araque A (2016) Activity-dependent switch of gabaergic inhibition into glutamatergic excitation in astrocyte-neuron networks. Elife 5:e20362.
Perea G, Navarrete M, Araque A (2009) Tripartite synapses: astrocytes process and control synaptic information. Trends Neurosci 32:421–431.
Perea G, Yang A, Boyden ES, Sur M (2014) Optogenetic astrocyte activation modulates response selectivity of visual cortex neurons in vivo. Nat Commun 5:3262.
Roth BL (2016) DREADDs for Neuroscientists. Neuron 89:683–694.
Santello M, Calì C, Bezzi P (2012) Gliotransmission and the tripartite synapse. In: Synaptic Plasticity, pp 307–331. Springer.
Serrano A, Haddjeri N, Lacaille J-C, Robitaille R (2006) GABAergic network activation of glial cells underlies hippocampal heterosynaptic depression. J Neurosci 26:5370–5382.
Sobieski C, Fitzpatrick MJ, Mennerick SJ (2017) Differential presynaptic ATP supply for basal and high-demand transmission. J Neurosci 37:1888–1899.
Srinivasan R, Huang BS, Venugopal S, Johnston AD, Chai H, Zeng H, Golshani P, Khakh BS (2015) Ca2+ signaling in astrocytes from Ip3r2 -/- mice in brain slices and during startle responses in vivo. Nat Neurosci 18:708–717.
Stobart JL, Ferrari KD, Barrett MJP, Glück C, Stobart MJ, Zuend M, Weber B (2018) Cortical circuit activity evokes rapid astrocyte calcium signals on a similar timescale to neurons. Neuron 98:726–735.
Tan Z, Liu Y, Xi W, Lou H, Zhu L, Guo Z, Mei L, Duan S (2017) Glia-derived ATP inversely regulates excitability of pyramidal and CCK-positive neurons. Nat Commun 8:13772.
Xie AX, Petravicz J, McCarthy KD (2015) Molecular approaches for manipulating astrocytic signaling in vivo. Front Cell Neurosci 9:144.
Yamashita A, Hamada A, Suhara Y, Kawabe R, Yanase M, Kuzumaki N, Narita M, Matsui R, Okano H, Narita M (2014) Astrocytic activation in the anterior cingulate cortex is critical for sleep disorder under neuropathic pain. Synapse 68:235–247.
Yang L, Qi Y, Yang Y (2015) Astrocytes control food intake by inhibiting AGRP neuron activity via adenosine A1 receptors. Cell Rep 11:798–807.

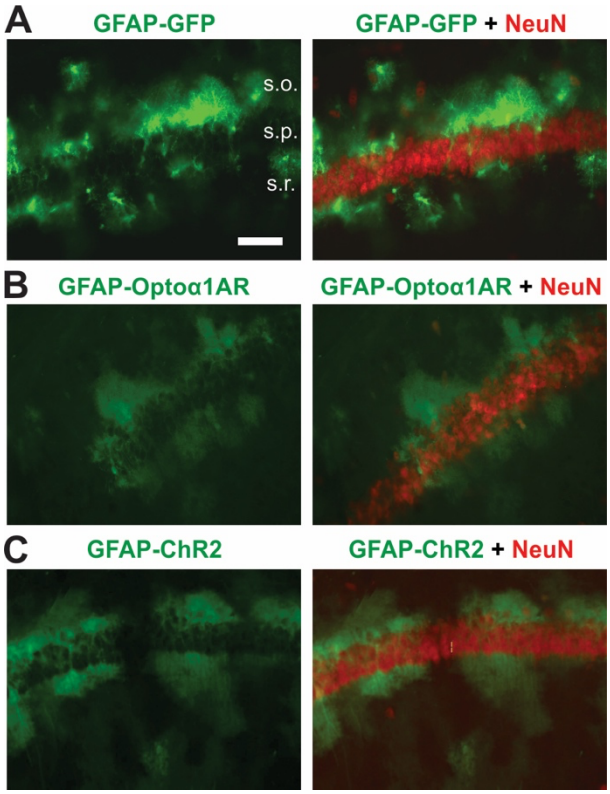

Figure 1 – AAV8-GFAP-Optoα1AR-eYFP selectively targets astrocytes in hippocampal CA1
Example immunohistochemical images displaying astrocytic targeting of optogenetic constructs.
(A) AAV8-GFAP-GFP (left) and AAV8-GFAP-GFP merged with neuronal marker NeuN (right). s.o., stratum oriens; s.p., stratum pyramidale; s.r., stratum radiatum. Scale bar, 40 µm
(B) AAV8-GFAP-Optoα1AR-eYFP (left) and AAV8-GFAP-Optoα1AR-eYFP merged with NeuN (right).
(C) AAV8-GFAP-hChR2(H134R)-eYFP (left), and AAV8-GFAP-hChR2(H134R)-eYFP merged with NeuN (right).

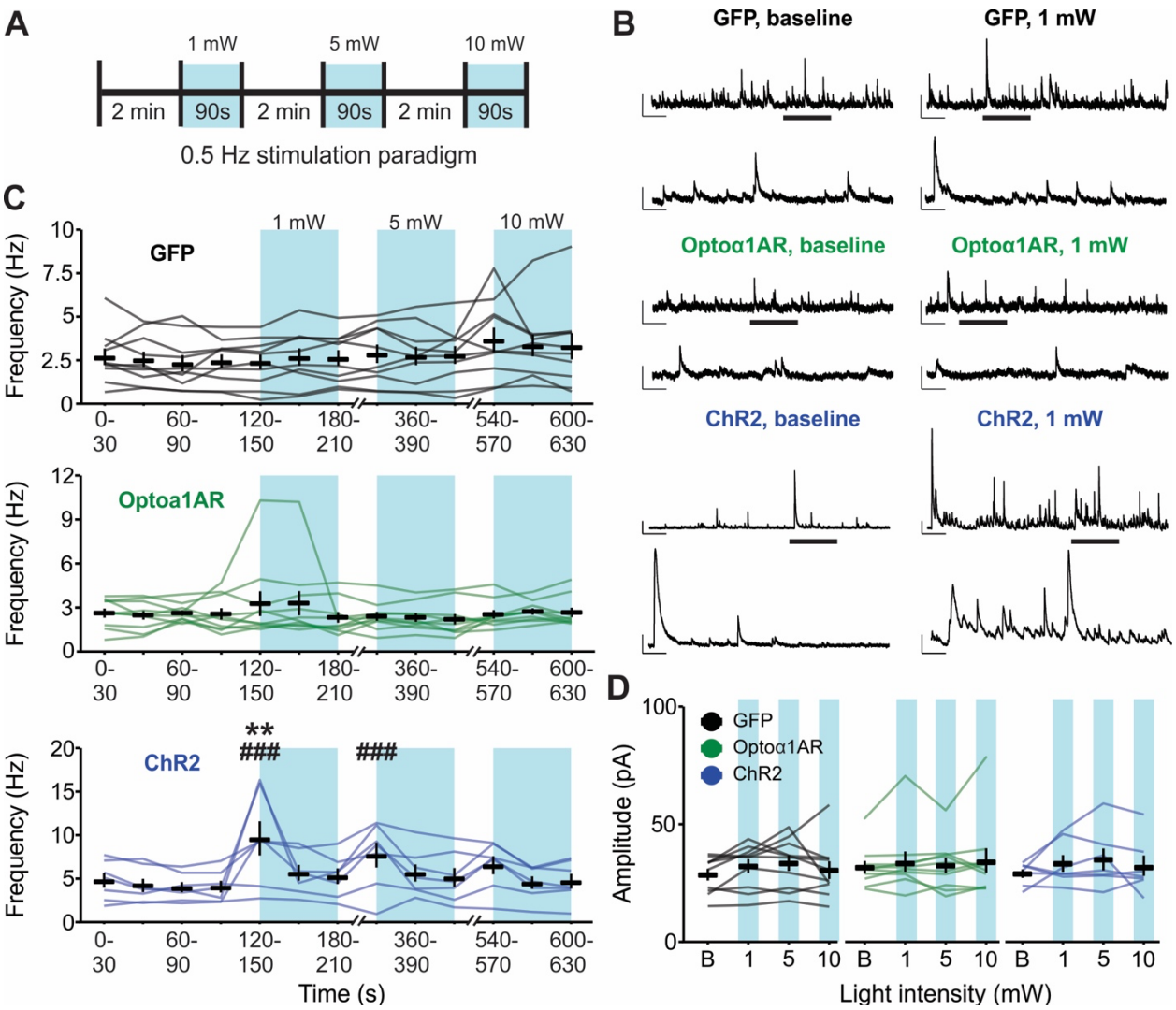

Figure 2 – Low-frequency (0.5 Hz) blue light stimulation of astrocytes expressing ChR2, but not Optoα1AR, increases sIPSC frequency

(A) Schematic representation of 0.5 Hz light stimulation paradigm.

(B) Representative sIPSC traces from individual pyramidal cells before (left) and during (right) 0.5 Hz blue light stimulation delivered to slices expressing GFP (top), Optoα1AR (middle), or ChR2 (bottom) in astrocytes. Insets represent expanded sections from underlined portion of trace. Scale bars – GFP and Optoα1AR: 50 pA, 1 s; inset: 50 pA, 200 ms; ChR2: 100 pA, 1s; inset: 100 pA, 200 ms.

(C) Mean ± SEM of sIPSC frequency across time of GFP (top), Optoα1AR (middle), and ChR2 (bottom) groups during 0.5 Hz stimulation. Lines represent individual cells. Note that lines are used to enable identification of the same cells across the time points; increased slope at end of baseline period does not represent an increase in frequency prior to light delivery.

(D) Mean ± SEM of sIPSC amplitude in GFP (left), Optoα1AR (middle), and ChR2 (right) groups across stimulation intensities. Lines represent individual cells. B = baseline.

**, $p<0.01$ vs. baseline values. ###, $p<0.001$ vs. GFP control group.

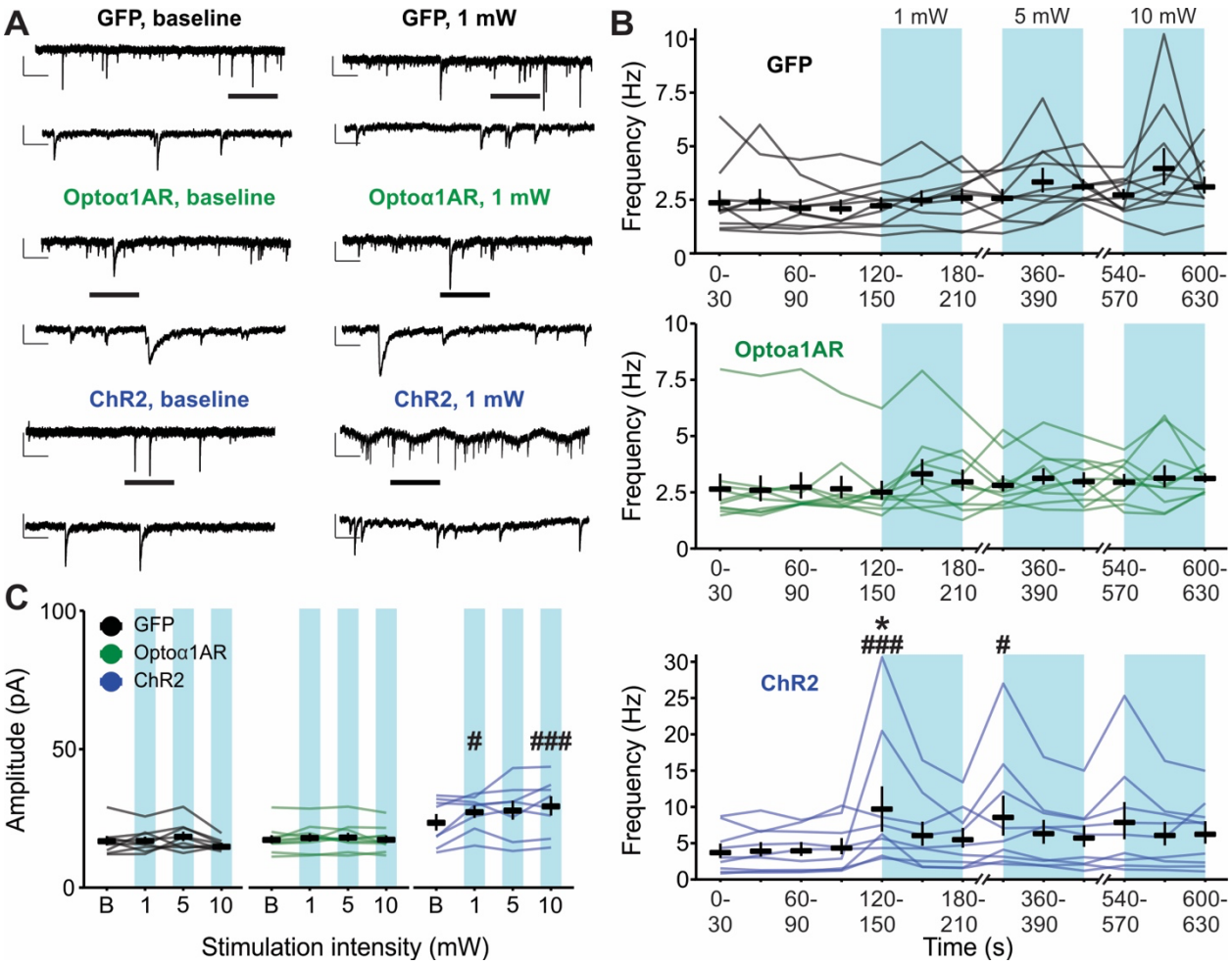

Figure 3 – Low-frequency (0.5 Hz) stimulation of astrocytes expressing ChR2, but not Optoα1AR, increases sEPSC frequency and amplitude

(A) Representative sEPSC traces from individual pyramidal cells before (left) and during (right) 0.5 Hz blue light stimulation delivered to slices expressing GFP (top), Optoα1AR (middle), or ChR2 (bottom) in astrocytes. Insets represent expanded sections from underlined portion of trace. Scale bars – GFP and Optoα1AR: 20 pA, 1 s; inset: 20 pA, 200 ms; ChR2: 50 pA, 1s; inset: 50 pA, 200 ms.

(B) Mean ± SEM of sEPSC frequency across time of GFP (top), Optoα1AR (middle), and ChR2 (bottom) groups during 0.5 Hz stimulation. Lines represent individual cells.

(C) Mean ± SEM of sEPSC amplitude of GFP (left), Optoα1AR (middle), and ChR2 (right) groups across stimulation intensities. Lines represent individual cells. B = baseline.

*, $p<0.05$ vs. baseline values. #, ###, $p<0.05$, $p<0.001$ vs. GFP control group.

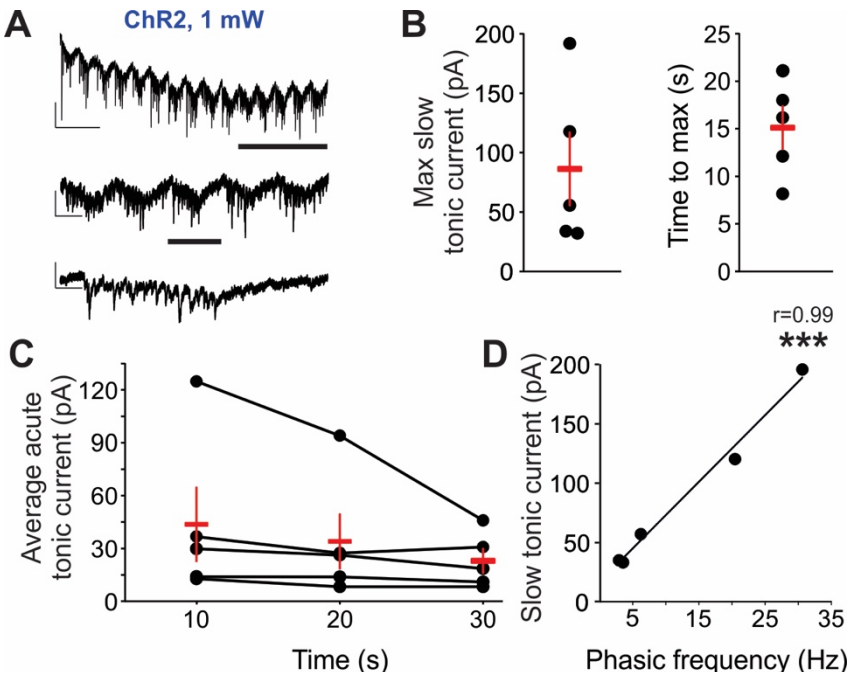

Figure 4 – Low-frequency (0.5 Hz) stimulation of astrocytes expressing ChR2 induces both slow and acute tonic inward currents.

(A) Representative sEPSC trace from an individual pyramidal cell during 0.5 Hz blue light stimulation delivered to slices expressing astrocytic ChR2. Insets represent expanded sections from underlined portion of trace. Scale bars: top, 50 pA, 5 s; middle: 50 pA, 1 s; bottom: 50 pA, 200 ms.

(B) Mean ± SEM (red markers) of the maximum amplitude of the slow tonic current (left) and time to max amplitude of slow tonic current (right). Dots represent individual cells (5 cells in which tonic currents were elicited, out of 9 recorded).

(C) Mean ± SEM (red markers) of the average acute tonic current during first 30 s of blue light exposure. Dots and connected lines represent individual cells.

(D) Slow tonic current amplitude plotted against the frequency of phasic sEPSCs in the same cells. Dots represent individual cells; linear regression line of best fit indicates strong correlation. *** $p<0.0001$, Pearson's correlation.

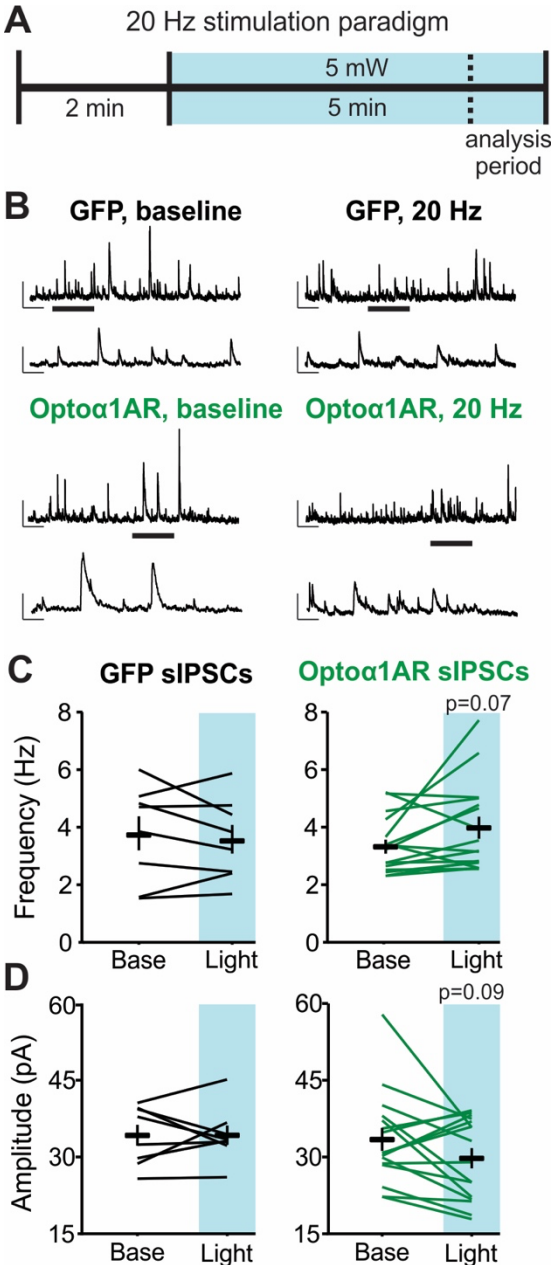

Figure 5 – High-frequency (20 Hz) stimulation of astrocytic Optoα1AR yields trends for increased sIPSC frequency and decreased sIPSC amplitude

(A) Schematic representation of 20 Hz stimulation paradigm.

(B) Representative sIPSC traces from individual pyramidal cells before (left) and during (right) 20 Hz stimulation of GFP (top) or Optoα1AR (bottom) in astrocytes. Insets represent expanded sections from underlined portion of trace. Scale bars: 50 pA, 1 s; inset: 50 pA, 200 ms.

(C) Mean ± SEM of sIPSC frequency before (Base) and during 20 Hz stimulation (Light) of GFP (left) or Optoα1AR (right) in astrocytes. Lines represent individual cells.

(D) Mean ± SEM of sIPSC amplitude before (Base) and during 20 Hz stimulation (Light) of GFP (left) or Optoα1AR (right) in astrocytes. Lines represent individual cells.

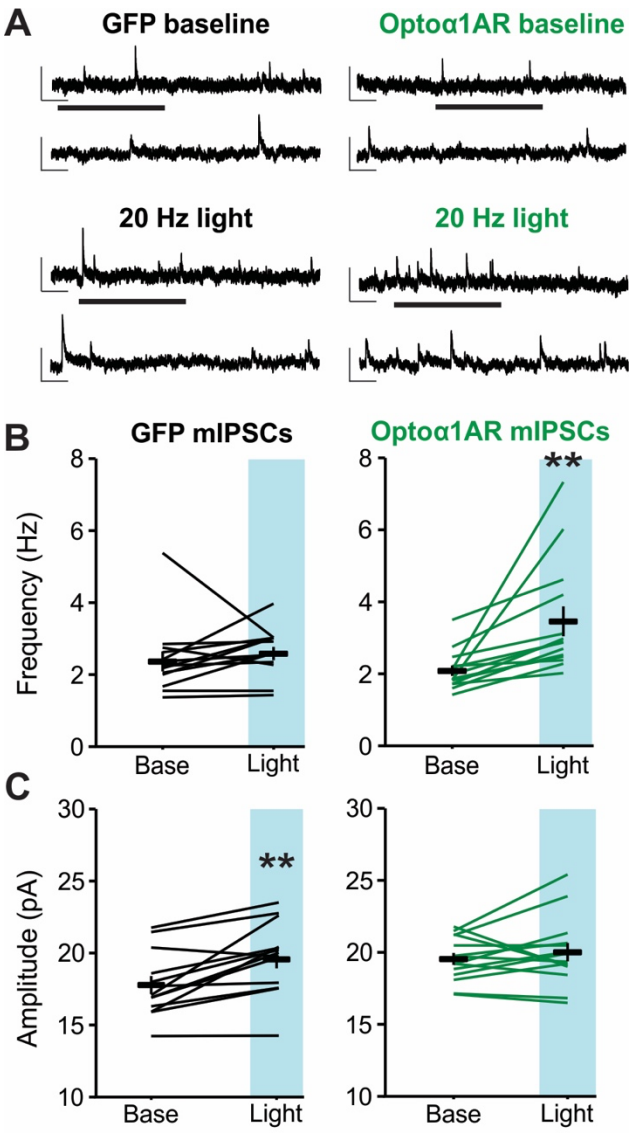

Figure 6 – High-frequency (20 Hz) stimulation of astrocytic Optoα1AR increases mIPSC frequency but does not affect mIPSC amplitude

(A) Representative mIPSC traces from individual pyramidal cells before (top) and during (bottom) 20 Hz stimulation of GFP (left) or Optoα1AR (right) in astrocytes. Insets represent expanded sections from underlined portion of trace. Scale bars: 20 pA, 500 ms; inset: 20 pA, 100 ms.

(B) Mean ± SEM of mIPSC frequency before (Base) and during 20 Hz stimulation (Light) of GFP (left) or Optoα1AR (right) in astrocytes. Lines represent individual cells.

(C) Mean ± SEM of mIPSC amplitude before (Base) and during 20 Hz stimulation (Light) of GFP (left) or Optoα1AR (right) in astrocytes. Lines represent individual cells.

**, $p<0.01$ vs. baseline value

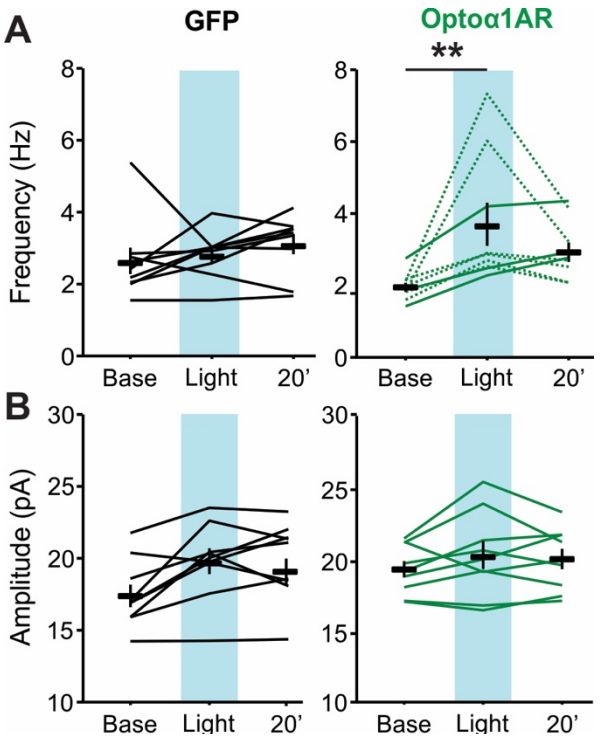

Figure 7 – Increase in mIPSC frequency with 20 Hz stimulation of Optoα1AR is reversible within 20 min after stimulation

(A) Mean ± SEM of mIPSC frequency before (Base), during 20 Hz stimulation (Light), and 20 minutes following 20 Hz stimulation (20') of GFP (left) or Optoα1AR (right) in astrocytes. Lines represent individual cells. Dotted lines represent 6 cells that showed reversibility of effect.

(B) Mean ± SEM of mIPSC amplitude before (Base), during 20 Hz stimulation (Light), and 20 minutes following 20 Hz stimulation (20') of GFP (left) or Optoα1AR (right) in astrocytes. Lines represent individual cells.

**, $p<0.01$ vs. baseline value

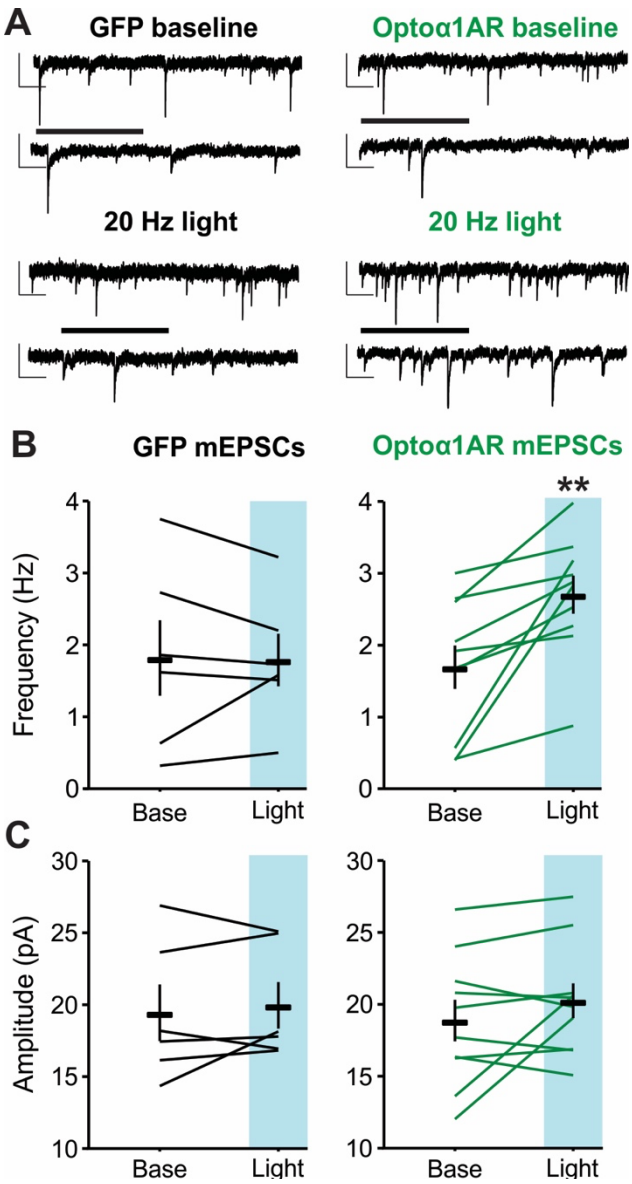

Figure 8 – High-frequency (20 Hz) stimulation of astrocytic Optoα1AR increases mEPSC frequency
(A) Representative mEPSC traces from individual pyramidal cells before (top) and during (bottom) 20 Hz stimulation of GFP (left) or Optoα1AR (right) in astrocytes. Insets represent expanded sections from underlined portion of trace. Scale bars: 20 pA, 500 ms; inset: 20 pA, 100 ms.
(B) Mean ± SEM of mEPSC frequency before (Base) and during 20 Hz stimulation (Light) of GFP (left) or Optoα1AR (right) in astrocytes. Lines represent individual cells.
(C) Mean ± SEM of mEPSC amplitude before (Base) and during 20 Hz stimulation (Light) of GFP (left) or Optoα1AR (right) in astrocytes. Lines represent individual cells.
**, $p<0.01$ vs. baseline value